

DVB-T/H and T-DMB: Physical Layer Performance Comparison in Fast Mobile Channels

Mario Poggioni, *Student Member, IEEE*, Luca Rugini, *Member, IEEE*, and Paolo Banelli, *Member, IEEE*

Abstract—Terrestrial or Handheld Digital Video Broadcasting (DVB-T/H) and Terrestrial Digital Multimedia Broadcasting (T-DMB) are two popular broadcasting standards that enable digital television transmissions to handheld receivers. This paper presents a comprehensive performance comparison between the physical layers of DVB-T/H and T-DMB when employed for mobile communications. By exploiting a recently proposed fast simulation model, we assess the BER of the two coded OFDM systems in several realistic scenarios, taking into account Rayleigh and Rice channels, different mobile speeds, inner and outer channel coding, channel estimation, and one or two receive antennas. Our comparison shows that the DVB-T/H physical layer performance highly depends on the delay spread of the channel, whereas T-DMB is less sensitive to the frequency selectivity of the channel. As a result, DVB-T/H yields better performance than T-DMB in typical Rayleigh channels with significant delay spread. On the contrary, at high SNR, T-DMB outperforms DVB-T/H in Rice channels with low delay spread. As a side result, we show the performance improvement of DVB-H produced by MPE-FEC at the data link layer.

Index Terms—BER performance, coded OFDM, DAB, Doppler spread, DVB-H, DVB-T, ICI, T-DMB, time-varying fading channels.

I. INTRODUCTION

DIGITAL Video Broadcasting (DVB) [1], with both Terrestrial (DVB-T) and Handheld (DVB-H) versions [2], and Digital Audio Broadcasting (DAB) [3], with its multimedia extension Terrestrial Digital Multimedia Broadcasting (T-DMB) [4], [5], are the two leading standards for multimedia broadcasting to mobile receivers. Initially, DAB and DVB were conceived for complementary tasks: DAB was intended for replacing analog audio transmissions, whereas DVB was designed for video signals, characterized by a larger bandwidth. However, due to the increased importance of multimedia broadcasting, T-DMB is actually a strong competitor of DVB-T/H, especially in those areas where DAB is already well developed. The availability of two different multimedia broadcasting standards raises an interesting issue about T-DMB and DVB-T/H: which one is to be preferred? In order to provide a meaningful

answer from the technological point of view, this paper compares the physical (PHY) layer performance of T-DMB and DVB-T/H in mobile scenarios.

We highlight that the PHY layers of T-DMB and DVB-T/H share some similarities, but have also many significant differences. Indeed, both standards are based on orthogonal frequency-division multiplexing (OFDM), but with different parameters, such as the number of subcarriers, their separation, and, consequently, the overall bit rate [1], [4]. Moreover, although both DVB and T-DMB commonly employ simple per-subcarrier equalization and demodulation that are optimal in time-invariant channels, in mobility conditions the intercarrier interference (ICI) due to Doppler spreading can produce a different impact on the bit-error rate (BER) performance, since DVB receivers usually perform coherent one-tap equalization, while DAB and T-DMB receivers often adopt differential demodulation [6], [7]. In addition, despite T-DMB and DVB-T/H employ similar frequency interleaving techniques, the time-interleaving span is very long in T-DMB, much shorter in DVB-H, and absent in DVB-T [1], with a consequent different coded BER even for the same uncoded BER [8]. As a result of the mentioned differences, a comparison of the *coded* BER of these broadcasting standards is of practical interest. Besides, DVB-H offers a further protection from Doppler effects at the data link (DL) layer, by means of multiprotocol encapsulation forward error correction (MPE-FEC).

A. Previous Literature and Work Motivation

Due to the popularity of DVB-T/H, DAB, and T-DMB, relevant investigations about the coded BER performance have been performed, e.g., in [6], [7], [9]–[12]. For instance, theoretical and simulated coded BER for DAB have been presented in [6] and [9]. However, the assumption of perfect interleaving produces a certain mismatch between theory and simulations, especially for high mobile speeds. Moreover, a theoretical extension to T-DMB seems difficult. On the other hand, coded BER simulation results for DVB-T are discussed in [7] and [10], including the effect of channel estimation. Specifically, [10] considers the interleaver effect but neglects the Doppler spreading, while [7] suggests the use of time interleaving, which is indeed included in DVB-H. Besides, the results of some field trials are summarized in [12], [13] for DAB and T-DMB, and in [7], [14]–[16] for DVB-T/H. In any case, most of the previous literature mainly focuses on a specific standard and avoids the comparison with alternative standards. Moreover, previous research studies assume different channel models and Doppler spread, which make it difficult to compare their results. Furthermore, possible differences between basic definitions (such as the signal-to-noise

Manuscript received November 05, 2008; revised September 25, 2009. First published October 30, 2009; current version published November 20, 2009.

The authors are with the Department of Electrical and Information Engineering, University of Perugia, Perugia 06125, Italy (e-mail: mario.poggioni@diei.unipg.it; luca.rugini@diei.unipg.it; paolo.banelli@diei.unipg.it).

Color versions of one or more of the figures in this paper are available online at <http://ieeexplore.ieee.org>.

Digital Object Identifier 10.1109/TBC.2009.2034418

ratio (SNR)) may introduce a significant bias into the comparison results. Therefore, to perform a fair comparison, this paper considers both DVB-T/H and T-DMB within the same framework, assuming the same channel model and using similar parameters. Similarly, DVB-T is compared with other two digital television broadcasting systems in [17].

B. Technical Approach for Performance Comparison

Ideally, the best approach to compare the BER performance of DVB-T/H and T-DMB would be using theoretical analyses, but unfortunately a closed-form BER derivation is very challenging, mainly because of two reasons. First, a major issue is the theoretical characterization of the Doppler effect on coded OFDM systems. Indeed, despite the Gaussian approximation of the ICI is useful to obtain the uncoded BER [18], the same model is inaccurate to predict the coded BER [19]. Second, the theoretical BER for convolutional codes over fading channels is very difficult to obtain, even in the absence of Doppler spread. Actually, closed-form BER expressions are available only for codes with low memory [20]; in addition, approximated expressions obtained from BER bounds, although tight for additive white Gaussian noise (AWGN) channels, are typically loose for fading channels [21]. As a consequence, at present, an accurate theoretical BER comparison between DVB-T/H and T-DMB looks unfeasible, and a simulation approach seems unavoidable.

On the other hand, when the channel is doubly selective, accurate coded BER simulations involve very long running times, mainly because of the high memory requirements caused by the interleavers, and because of the high number of runs to average over the channel statistics. As a consequence, the number of simulation scenarios would be rather limited. To reduce this problem, we adopt two fast but accurate simulation models. The first one, known as equivalent frequency-domain OFDM model (EFDOM), is specifically tailored to DVB-T/H, and has been derived and validated in [19]. The second model, which is exploited for T-DMB, is a simple combination of the EFDOM with the well-known block fading model. These two models permit to simulate the coded BER in a reasonable time, thereby extending the number of considered scenarios.

C. Paper Structure and Notation

The rest of this paper is organized as follows. Section II introduces the OFDM system model in time-varying channels, and briefly reviews the PHY layers of DVB-T/H and T-DMB. Section III presents the simulation scenario and our main assumptions. Section IV describes DVB-T/H channel estimation, while Section V extends the comparison to multiple receive antennas. Section VI is devoted to simulation results and discussion, and Section VII concludes the paper.

We use the following notation. Bold uppercase (lowercase) letters denote matrices (column vectors); the superscripts $*$, T , H , $^{-1}$ denote conjugation, transpose, Hermitian, and inverse, respectively. \mathbf{I}_K stands for the identity matrix of size K , while $\mathbf{0}_{M \times N}$ is the $M \times N$ all-zero matrix. $[\mathbf{x}]_i$ denotes the i th element of \mathbf{x} , $\text{Diag}(\mathbf{a})$ is a diagonal matrix with \mathbf{a} on its diagonal, whereas $\text{diag}(\mathbf{A})$ is the column vector containing the main diagonal of the square matrix \mathbf{A} . Finally, $\lfloor a \rfloor$ denotes the integer floor function applied to the real number a .

II. SYSTEM MODEL

A. Time-Varying Multipath Channels

We consider a time-varying multipath channel obtained by discrete-time sampling of a continuous-time channel. Since time variation implies time-selective fading, while multipath implies frequency-selective fading, we are actually considering discrete-time doubly-selective fading channels. The time evolution of the l th channel path is expressed by

$$h_l[k] = h_c(kT_S, lT_S), \quad l = 0, \dots, L-1, \quad (1)$$

where the continuous-time channel $h_c(t, \tau)$ is wide-sense stationary with uncorrelated scattering (WSSUS) [22], $L = \lfloor \tau_{MAX}/T_S \rfloor + 1$ is the number of discrete channel paths, τ_{MAX} is the maximum excess delay, T_S is the sampling period, $\{\sigma_l^2 = E\{|h_l[k]|^2\}, l = 0, \dots, L-1\}$ represents the power-delay profile (PDP) and k denotes the discrete-time temporal index.

B. OFDM System Model

We consider an OFDM system with N subcarriers and cyclic prefix (CP) of length $L_{CP} \geq L-1$. Consequently, there is no inter-block interference (IBI) and the received signal, after CP removal and fast Fourier transform (FFT), can be written as [23]

$$\begin{aligned} \mathbf{y}(n) &= \mathbf{F}\tilde{\mathbf{H}}(n)\mathbf{F}^H\mathbf{x}(n) + \mathbf{F}\mathbf{w}(n) \\ &= \mathbf{H}(n)\mathbf{x}(n) + \mathbf{v}(n), \end{aligned} \quad (2)$$

where $\mathbf{H}(n) = \mathbf{F}\tilde{\mathbf{H}}(n)\mathbf{F}^H$, $\tilde{\mathbf{H}}(n)$ is the channel matrix in the time domain, \mathbf{F} is the unitary DFT matrix of size N , and n is the index of the OFDM block. Thus, the frequency-domain noise $\mathbf{v}(n)$ has the same statistics of the time-domain AWGN $\mathbf{w}(n)$. The $N \times 1$ transmitted signal $\mathbf{x}(n)$ is obtained from the N_D -dimensional QAM data signal by inserting the N_P pilots, the N_{TPS} Transmission Parameter Signaling (TPS) subcarriers¹ [1] and the N_G switched-off guard subcarriers. We also define N_A as the number of active subcarriers, with $N_A = N - N_G = N_D + N_P + N_{TPS}$. In T-DMB, $N_P = N_{TPS} = 0$.

Typically, OFDM systems employ per-subcarrier equalization assuming $\mathbf{H}(n)$ as diagonal, as it occurs when the channel is time invariant. On the contrary, time-varying channels introduce ICI that renders $\mathbf{H}(n)$ non-diagonal [18]. By separating the time-invariant part of the channel from its time-varying part, we have

$$\begin{aligned} \tilde{\mathbf{H}}(n) &= \tilde{\mathbf{H}}_U(n) + \tilde{\mathbf{H}}_I(n), \\ \mathbf{H}(n) &= \mathbf{H}_U(n) + \mathbf{H}_I(n), \end{aligned} \quad (3)$$

where $\tilde{\mathbf{H}}_U(n)$ is the time-domain circulant matrix that contains (on its first L diagonals) the elements of the average channel vector $\tilde{\mathbf{h}}_T(n)$ during the n th OFDM block, expressed by $\tilde{\mathbf{h}}_T(n) = 1/N \sum_{k=L_{CP}}^{N+L_{CP}-1} \mathbf{h}_T(k + n(N + L_{CP}))$, where $\mathbf{h}_T(k + n(N + L_{CP})) = [h_0(k + n(N + L_{CP})), \dots, h_{L-1}(k +$

¹Our detector does not consider the TPS subcarriers, which however are inserted because they contribute to the ICI power.

$n(N + L_{CP})]^T$, while $\tilde{\mathbf{H}}_I(n)$ represents the time-varying part of the channel. In (3), the matrices $\mathbf{H}_U(n) = \mathbf{F}\tilde{\mathbf{H}}_U(n)\mathbf{F}^H$ and $\mathbf{H}_I(n) = \mathbf{F}\tilde{\mathbf{H}}_I(n)\mathbf{F}^H$ have the following properties:

$$\begin{aligned} \mathbf{H}_U(n) &= \text{Diag}\left(\sqrt{N}\mathbf{F}\tilde{\mathbf{h}}_T(n)\right), \\ \text{diag}(\mathbf{H}_I(n)) &= \mathbf{0}_{N \times 1}. \end{aligned} \quad (4)$$

Inserting (3) in (2), we obtain

$$\begin{aligned} \mathbf{y}(n) &= \mathbf{y}_U(n) + \mathbf{i}(n) + \mathbf{v}(n) \\ &= \mathbf{H}_U(n)\mathbf{x}(n) + \mathbf{H}_I(n)\mathbf{x}(n) + \mathbf{v}(n), \end{aligned} \quad (5)$$

where $\mathbf{y}_U(n) = \mathbf{H}_U(n)\mathbf{x}(n)$ and $\mathbf{i}(n) = \mathbf{H}_I(n)\mathbf{x}(n)$ represent the useful received signal and the ICI, respectively, in the frequency domain.

In order to estimate the *uncoded* BER, it is widely acknowledged that the ICI can be accurately modeled as an additional AWGN with power [24]

$$P_{ICI} = 1 - \frac{1}{N^2} \left(N + 2 \sum_{i=1}^{N-1} i J_0 \left(2\pi \frac{\bar{f}_D}{N} (N - i) \right) \right), \quad (6)$$

where $J_0(\cdot)$ is the zero-order Bessel function of the first kind, i is the subcarrier index, and $\bar{f}_D = (f_D/\Delta f) = NT_S f_C (v/c)$ is the normalized Doppler spread, where f_D is the absolute Doppler spread, Δf is the subcarrier separation, f_C is the carrier frequency, c is the speed of light, and v is the speed of the mobile receiver in the transmit antenna direction. However the AWGN-like ICI model is not sufficient to characterize the *coded* BER [19]. This means that the ICI cannot be replaced by an additional AWGN with power P_{ICI} . As a consequence, more refined models, such as those described in Section III, are necessary.

C. Channel Coding and Interleaving

DVB-T/H employs a concatenated code: the outer code is a (204, 188) shortened systematic Reed-Solomon (RS) code, while the inner code is a rate-compatible punctured convolutional (RCPC) code [1] with polynomial generators $G = [171, 133]$ in octal form, and constraint length $\kappa = 7$. On the contrary, DAB only has an RCPC code with $G = [133, 171, 145, 133]$ and $\kappa = 7$ [3]. Therefore, the DVB-T/H inner code can be obtained by puncturing the DAB code. A concatenated code is used also for T-DMB, where the RCPC code of DAB is used as inner code, and the RS code of DVB-T/H is used as outer code [4].

The interleaving strategies of DVB-T/H and T-DMB are significantly different. In DVB-T/H, the outer convolutional interleaving acts on the *bytes* at the output of the RS encoder, while the inner interleaver scrambles the *bits* at the output of RCPC encoder. The inner interleaver depends on the DVB standard and mode: in DVB-T Mode 2k, there is only a frequency interleaving, with the same rule for all OFDM symbols; on the contrary, in DVB-H Mode 2k, there is also a time-frequency in-depth inner interleaver that works on QAM symbols

belonging to 4 consecutive OFDM symbols [1]. The inner interleaved data vector can be expressed by

$$\begin{aligned} \mathbf{x}_{sym}(n) &= \mathbf{P}_{DVB-T} \mathbf{x}_{bit}(n), n \in \mathbb{N}, \\ \mathbf{x}_{sym}(m) &= \mathbf{P}_{DVB-H} \left[\mathbf{x}_{bit}^T(4m+1), \mathbf{x}_{bit}^T(4m+2), \right. \\ &\quad \left. \mathbf{x}_{bit}^T(4m+3), \mathbf{x}_{bit}^T(4m+4) \right]^T, m \in \mathbb{N}_0, \end{aligned} \quad (7)$$

for DVB-T and DVB-H, respectively, where $\mathbf{x}_{bit}(n)$ is the $N_D \times 1$ OFDM symbol before the bit interleaver, and \mathbf{P}_{DVB-T} and \mathbf{P}_{DVB-H} are suitable permutation matrices [1].

T-DMB employs the same outer convolutional interleaving of DVB-T/H, while the inner interleaver is the same of DAB, described in the following. DAB Mode III has separate frequency and time inner interleaving: the frequency inner interleaver is similar to the DVB-T inner interleaver, with the same rule for all the OFDM symbols, whereas the time inner interleaver is more complicated and spans a long time interval of 320 ms (i.e., 2160 OFDM symbols) [3].

III. SIMULATION MODEL

A. Channel Models for Simulations

DVB-T/H provides for a specific simulation channel model [1], which however is deterministic and hence not suitable for mobile scenarios. Therefore, we employ channel models defined for mobile scenarios, taken from the COST 207 [25]. In COST 207, channel models are first defined as continuous-time models, and subsequently approximated by discrete-time models with reduced number of channel taps [25]. Since DVB-T/H and T-DMB have different symbol periods, we choose the non-approximated continuous-time models, and we obtain the discrete-time PDP by sampling the continuous-time PDP.

Specifically, we focus on the Bad Urban (BU) model, whose taps follow a Rayleigh statistic, and the Rural Area (RA) model, for Rice channels. For the BU model, the PDP is $P(\tau) = e^{-\tau}$ for $0 \leq \tau < 5$, $P(\tau) = 0.5e^{5-\tau}$ for $5 \leq \tau < 10$, and $P(\tau) = 0$ elsewhere, with τ in microseconds [25]. Hence, σ_l^2 is evaluated as $\sigma_l^2 = P(lT_S) / \sum_{i=0}^{L-1} P(iT_S)$. The number L of channel taps depends on the sampling time T_S and is therefore different for the two standards. For the RA model, the line-of-sight (LOS) component is at $\tau = 0$, while the non-LOS (NLOS) part of the PDP is $P(\tau) = e^{-9.2\tau}$ for $0 \leq \tau < 0.7$, and $P(\tau) = 0$ elsewhere [25]. The time variation of the channel paths, with Jakes' Doppler spectrum, is obtained by the sum-of-sinusoids method of [26].

B. Simulation Scenarios

To focus our comparison, we make some choices about the simulation scenarios and parameters, as follows.

C0) In both DVB-T/H and T-DMB, we consider the transmission modes with lowest FFT size, i.e., the DVB-T/H Mode 2k ($N = 2048$) and the T-DMB Mode III ($N = 256$). Indeed, since the bandwidth is fixed, the lowest FFT size corresponds to

the largest subcarrier spacing, i.e., the greatest robustness to the high Doppler spreads we consider. For DVB-T/H Mode 2k, the number of active subcarriers is $N_A = 1705$, and therefore the subcarrier separation is $\Delta f \approx 4.46$ kHz (2.79 kHz) when the bandwidth is $B \approx 7.6$ MHz (4.8 MHz). For T-DMB Mode III, $\Delta f = 8$ kHz, since $N_A = 192$ and $B = 1.536$ MHz.

C1) In DVB-T/H, we focus on QPSK only. Indeed, in the highly mobile scenarios we focus on, one-tap equalization of higher-order QAM performs poorly. Besides, since T-DMB uses DQPSK, this choice produces a similar Viterbi decoding complexity for both standards.

C2) For each standard, we choose the CP length and the code rates that yield similar spectral efficiencies. For instance, DVB-T/H with CP duration $T_{CP} = T_U/16$ produces a spectral efficiency $\eta \approx 0.77$ bps/Hz ($\eta \approx 1.03$ bps/Hz) when the code rate (CR) of the convolutional code is $r = 1/2$ ($r = 2/3$). On the other hand, using T-DMB with CP duration $T_{CP} \approx T_U/4$ leads to $\eta \approx 0.74$ ($\eta \approx 0.98$) bps/Hz when the CR of the convolutional code is $r = 1/2$ ($r = 2/3$). The spectral efficiency herein calculated only considers the useful bandwidth B (guard subcarriers are excluded).

C3) To guarantee fairness, we use the same carrier frequency f_C for both standards. We consider both $f_C = 800$ MHz and $f_C = 1.4$ GHz, which are typical values for DVB-T/H and T-DMB, respectively.

C4) In the DVB-T/H receiver, we include a simple channel estimator. Indeed, T-DMB usually employs DQPSK differential demodulation that implicitly estimates the channel.

C5) In both receivers, we consider a soft Viterbi decoder with 4-bits quantization. For T-DMB, before quantization, we use a μ -law compander, which is not useful for DVB-T/H.

C. DVB-T/H Simulation Model

To assess the coded BER of DVB-T/H, we exploit a fast simulation model known as *EFDOM* [19]. In DVB-T, the EFDOM replaces (5) with

$$\mathbf{y}(n) = \mathbf{A}(n)\mathbf{x}(n) + \mathbf{i}^{(E)}(n) + \mathbf{v}(n), \quad (8)$$

where $\mathbf{A}(n)$ is the $N \times N$ useful channel diagonal matrix, $\mathbf{i}^{(E)}(n)$ represents the ICI, and $\mathbf{v}(n)$ is the AWGN, in the n th block. Due to the DVB-T interleaver length, each OFDM symbol can be simulated separately, and $\mathbf{A}(n)$ and $\mathbf{i}^{(E)}(n)$ are independently generated. The specific feature of the EFDOM is the fast generation of $\mathbf{i}^{(E)}(n)$, which is not the exact ICI $\mathbf{i}(n)$ of (5) generated by the channel time variation, but it represents the effective amount of ICI that produces the same coded BER performance caused by the exact ICI [19].

For DVB-H, where the time inner interleaver spans a superblock of 4 consecutive OFDM blocks, the EFDOM is expressed as

$$\underline{\mathbf{y}}(m) = \underline{\mathbf{A}}(m)\underline{\mathbf{x}}(m) + \underline{\mathbf{i}}^{(E)}(m) + \underline{\mathbf{v}}(m), \quad (9)$$

where $\underline{\mathbf{y}}(m)$ and $\underline{\mathbf{x}}(m)$ are $4N \times 1$ vectors representing the received and transmitted signals, respectively, while $\underline{\mathbf{A}}(m)$ is a $4N \times 4N$ diagonal matrix representing the time-invariant part of the channel, and $\underline{\mathbf{i}}^{(E)}(m)$ and $\underline{\mathbf{v}}(m)$ are the ICI and AWGN, respectively, in the m th superblock. In this case, to preserve the

same coded BER of the exact system, the EFDOM requires a joint generation of $\underline{\mathbf{A}}(m)$ and $\underline{\mathbf{i}}^{(E)}(m)$ [19].

D. DAB and T-DMB Simulation Model

For DAB and T-DMB, due to the long time interleaver, the EFDOM would be unmanageable, since $\underline{\mathbf{A}}(m)$ would have size $2160N \times 2160N$. Anyway, we can efficiently simulate the time-varying channel by exploiting a simple block-fading model, introducing a suitable temporal correlation among the blocks. In other words, the time-varying channel is approximated as time invariant within the OFDM block, maintaining the time variation from block to block. This way, the complexity of the channel generation is reduced of a factor $N + L_{CP}$. This correlated block-fading model, denoted with *simplified EFDOM*, is expressed by

$$\mathbf{y}(n) = \mathbf{B}(n)\mathbf{x}(n) + \mathbf{i}^{(B)}(n) + \mathbf{v}(n), \quad (10)$$

where $\mathbf{i}^{(B)}(n)$ and $\mathbf{v}(n)$ are $N \times 1$ vectors representing the ICI and the AWGN, respectively, in the n th OFDM block, while $\mathbf{B}(n)$ is the $N \times N$ frequency-domain diagonal matrix that contains a randomly generated time-invariant channel realization with the same PDP of $\mathbf{h}_T(n)$. The time variation from block to block is generated as in [26] using the block-normalized Doppler frequency $\tilde{f}_D = (N + L_{CP})\frac{f_D}{N}$.

Differently from the EFDOM used for DVB-T/H, the simplified EFDOM for DAB and T-DMB only approximates the correlation between the channel values of different OFDM blocks. Anyway, there exists a close agreement between the coded BER of the exact DAB and of the simplified model [27]. This good accuracy is maintained in the T-DMB case, which also includes RS outer coding.

IV. DVB CHANNEL ESTIMATION AND EQUALIZATION

In DVB-T/H systems, pilot-aided channel estimation can exploit fixed and scattered pilot subcarriers [1]. We only consider the $N_S(n)$ scattered pilots, with pilot indexes in $I_S(n) = \{i \in \mathbb{N}_0 : i = 3(n_{\text{mod}4}) + 12p, p \in \mathbb{N}_0, i < N_A\}$, because their regular spacing simplifies the channel estimation. For convenience, we express the $N_A \times 1$ transmitted vector as

$$\bar{\mathbf{x}}(n) = \bar{\mathbf{x}}_D(n) + \bar{\mathbf{x}}_S(n) + \bar{\mathbf{x}}_{OT}(n), \quad (11)$$

where $\bar{\mathbf{x}}_D(n)$ is the data vector, $\bar{\mathbf{x}}_S(n)$ is the vector of scattered pilots, and $\bar{\mathbf{x}}_{OT}(n)$ is the vector that contains both unused pilots and TPS. In (11), $\bar{\mathbf{x}}_D(n)$ is obtained by inserting the N_D elements of $\mathbf{x}_{\text{sym}}(n)$ in the N_D data positions, while the remaining $N_A - N_D$ elements are zero. Similarly, $[\bar{\mathbf{x}}_S(n)]_i$ is nonzero only when $i \in I_S(n)$, and its value is $\pm 4/3$ as defined in [1]. In the same way, $\bar{\mathbf{x}}_{OT}(n)$ has $N_O(n) + N_{TPS}$ nonzero elements, where $N_O(n) = N_P - N_S(n)$ is the number of pilot subcarriers we do not use in the channel estimation. Actually, $\bar{\mathbf{x}}(n)$ in (11) is the transmitted vector in (5) after the guard band removal, as expressed by $\bar{\mathbf{x}}(n) = \mathbf{G}\mathbf{x}(n)$, where \mathbf{G} is the $N_A \times N$ matrix that removes the N_G guard subcarriers.

Many pilot-aided equalization techniques have been proposed for OFDM in doubly-selective channels [28], which however require a complex time-variant channel estimation.

Aiming at low complexity, we focus on time-invariant equalization techniques developed for low Doppler scenarios [29], [30]. For the same reason, we avoid two-dimensional channel estimation methods [31], and we consider frequency-domain interpolation techniques that estimate $\mathbf{h}(n) = \text{diag}(\mathbf{H}_U(n))$.

A. Linear Interpolation

Linear interpolation (LI) is simple and widely employed in commercial devices. In this case, for each subcarrier, the frequency-domain channel response is obtained by a weighted average of the values estimated on the two closest pilot subcarriers [32].

B. Least-Squares Fitting

Least-squares (LS) fitting produces the maximum-likelihood estimate [29] and the minimum variance unbiased estimate [33], when a unique OFDM block is used, without prior knowledge about channel and noise statistics. LS fitting works on a sub-vector $\mathbf{y}_S(n)$ expressed by

$$\mathbf{y}_S(n) = \text{Diag}(\mathbf{S}(n)\bar{\mathbf{x}}_S(n))^{-1} \mathbf{S}(n)\mathbf{G}\mathbf{y}(n), \quad (12)$$

where $\mathbf{S}(n)$ is the $N_S(n) \times N_A$ submatrix of \mathbf{I}_{N_A} that selects the elements corresponding to the $N_S(n)$ scattered pilot positions. Typically, the channel length L is assumed known [32]. Therefore, we define the matrix $\mathbf{F}_L = \mathbf{G}\mathbf{F}[\mathbf{I}_L, \mathbf{0}_{L \times (N-L)}]^T$, which contains the first L columns of $\mathbf{G}\mathbf{F}$, and its submatrix $\mathbf{F}_{S,L}(n)$, which contains the $N_S(n)$ rows of \mathbf{F}_L corresponding to the scattered pilot positions. By these definitions, the LS frequency-domain channel estimate is expressed by

$$\hat{\mathbf{h}}_{LS}(n) = \mathbf{F}_L (\mathbf{F}_{S,L}^H(n)\mathbf{F}_{S,L}(n))^{-1} \mathbf{F}_{S,L}^H(n)\mathbf{y}_S(n). \quad (13)$$

Clearly, the matrix inverse can be precomputed and stored.

C. Cardinal Interpolation

Cardinal interpolation (CI) is a trade-off between the simplicity of LI and the good performance of LS fitting. In this case, the frequency-domain channel estimate is obtained as

$$\hat{\mathbf{h}}_{CI}(n) = 12\mathbf{F}_L\mathbf{F}_{S,L}^H(n)\mathbf{y}_S(n). \quad (14)$$

CI corresponds to frequency-domain zero filling plus IDFT, represented by $\mathbf{F}_{S,L}^H(n)$, and a subsequent \mathbf{F}_L , which removes the time-domain replicas introduced by zero filling and performs a DFT to come back in the frequency domain. Please observe that CI is less complex than LS fitting, since it does not require any matrix inverse. Moreover, differently from LI, CI leads to a perfect estimate in the absence of noise and ICI, as long as $L \leq N/12$, due to the Nyquist-Shannon theorem.

D. Equalization

Since we focus on QPSK, we compensate only for the estimated phase of the channel, as expressed by

$$[\hat{\mathbf{x}}_{EQ}(n)]_i = [\mathbf{y}(n)]_i e^{-j\angle[\hat{\mathbf{h}}(n)]_i}, \quad (15)$$

where $\hat{\mathbf{x}}_{EQ}(n)$ is the equalized OFDM symbol, $\hat{\mathbf{h}}(n)$ is the channel estimate, and i is the subcarrier index. This way, the

equalized data is weighted by the channel gain, which is a reliability index that can be exploited by soft convolutional decoding techniques [34].

V. RECEIVER DIVERSITY

In this section, we extend our comparison between DVB-T/H and T-DMB to multiantenna devices. Specifically, we consider the spatial diversity at the receiver, which can greatly enhance the BER performance, while preserving low complexity. Motivated by practical implementation constraints, we consider only two receive antennas.

In DVB-T/H, we exploit the spatial diversity by maximal-ratio combining (MRC), which is known to be SNR-optimal for perfect channel estimation and in absence of ICI [35]. Thus, we express the MRC output as

$$\hat{\mathbf{x}}_{MRC}(n) = \left(\hat{\mathbf{H}}_1^H(n)\hat{\mathbf{H}}_1(n) + \hat{\mathbf{H}}_2^H(n)\hat{\mathbf{H}}_2(n) \right)^{-1} \left(\hat{\mathbf{H}}_1^H(n)\mathbf{y}_1(n) + \hat{\mathbf{H}}_2^H(n)\mathbf{y}_2(n) \right), \quad (16)$$

where we use subscripts to distinguish the two antenna channels, and the superscript $\hat{\cdot}$ to denote an estimate. Since the matrices $\hat{\mathbf{H}}_1(n)$ and $\hat{\mathbf{H}}_2(n)$ are diagonal, the MRC in (16) is done on a per-subcarrier basis, which induces a limited complexity increase.

On the other hand, in T-DMB, due to the differential demodulation, the channel estimate is not available, and consequently MRC cannot be used. However, other combining techniques are possible [36]. In this paper, we consider the equal-gain combining (EGC), which captures almost the same diversity of MRC [37]. The EGC output is expressed by

$$\hat{\mathbf{x}}_{EGC}(n) = \frac{1}{2} \{ \mathbf{y}_1^*(n-1) \odot \mathbf{y}_1(n) + \mathbf{y}_2^*(n-1) \odot \mathbf{y}_2(n) \}, \quad (17)$$

where \odot stands for the element-wise product. Clearly, per-subcarrier processing and low complexity are maintained.

To assess the BER performance, we have to generate two spatially correlated channels $h_{l,1}[k]$ and $h_{l,2}[k]$, where l is the channel tap index and k is the time index. This is done by imposing to the spatial channel vector $\mathbf{h}_l[k] = [h_{l,1}[k], h_{l,2}[k]]^T$ a covariance matrix \mathbf{C} equal to

$$\mathbf{C} = E \{ \mathbf{h}_l[k]\mathbf{h}_l^H[k] \} = \begin{bmatrix} 1 & \rho \\ \rho & 1 \end{bmatrix}, \quad (18)$$

where for simplicity we have assumed ρ as real. In this view, the two spatially correlated channels are generated from two independent auxiliary channels $\check{h}_{l,1}[k]$ and $\check{h}_{l,2}[k]$ as

$$\begin{bmatrix} h_{l,1}[k] \\ h_{l,2}[k] \end{bmatrix} = \frac{\sqrt{2}}{2} \begin{bmatrix} \sqrt{1+\rho} & -\sqrt{1-\rho} \\ \sqrt{1+\rho} & \sqrt{1-\rho} \end{bmatrix} \begin{bmatrix} \check{h}_{l,1}[k] \\ \check{h}_{l,2}[k] \end{bmatrix}. \quad (19)$$

VI. COMPARISON BETWEEN DVB-T/H AND T-DMB

In our comparison, we mainly monitor the coded BER, at the output of either the Viterbi decoder or the outer RS decoder. Although we focus on the PHY layer, in a few cases we also consider the DL layer BER performance at the output of the

TABLE I
SYSTEM PARAMETERS

	T-DMB Mode III	DVB-T/H 2k @ 5 MHz	DVB-T/H 2k @ 8 MHz
FFT size N	256	2048	2048
Active subcarriers N_A	192	1705	1705
Data subcarriers N_D	192	1512	1512
Bandwidth B (MHz)	1.536	4.7573	7.6116
Channel separation B_c (MHz)	1.75	5.00	8.00
Subcarrier spacing Δf (kHz)	8.00	2.79	4.46
Sampling frequency f_s (MHz)	2.048	5.714	9.143
Block duration T_U (μ s)	125.00	358.40	224.00
CP duration T_{CP} (μ s)	31.00	22.40	14.00
Modulation	$\pi/4$ -DQPSK	QPSK	QPSK
Bit rate r_b (Mbps) (CR $r = 1/2$)	1.1342	3.6592	5.8547
Bit rate r_b (Mbps) (CR $r = 2/3$)	1.5123	4.8789	7.8062
Spectral efficiency η (bps/Hz) (CR $r = 1/2$)	0.7384	0.7692	0.7692
Spectral efficiency η (bps/Hz) (CR $r = 2/3$)	0.9846	1.0256	1.0256

MPE-FEC decoder. The system parameters we focused on, are summarized in Table I.

A. Rayleigh Channels With High Delay Spread

Fig. 1 shows the BER at the output of the Viterbi decoder of T-DMB and DVB-H (8 MHz) systems in the Rayleigh BU channel, for a mobile speed $v = 150$ km/h and a carrier frequency $f_C = 800$ MHz. This corresponds to a normalized Doppler spread $\bar{f}_D \approx 1.9\%$ for T-DMB, and $\bar{f}_D \approx 2.5\%$ for DVB-H. For comparison purposes, we include the BER obtained when $v = 0$ km/h, i.e., in time-invariant channels, denoted with “TI” in Fig. 1. Please note that this inner T-DMB system (inner convolutional code without outer RS coding) corresponds to a DAB physical layer. The SNR for any data subcarrier is defined at the FFT output (2). Fig. 1 displays that, when $v = 150$ km/h and the convolutional CR is $r = 1/2$, DVB-H with LI performs similarly to T-DMB. Specifically, T-DMB outperforms DVB-H at high SNR, while DVB-H presents a performance advantage at low SNR. On the contrary, when the convolutional CR is $r = 2/3$, T-DMB outperforms DVB-H at low SNR. However, it should be noted that the LI channel estimation penalizes DVB-H, with an SNR penalty of roughly 3 dB with respect to ideal channel state information (ICSI). It is interesting to note that, in case of fixed reception (i.e., without mobility), DVB-H exhibits a better BER performance than in mobility scenarios, because of the absence of the ICI; on the other hand, in fixed scenarios, T-DMB presents a much worse BER than in mobility conditions (2 dB SNR loss), because T-DMB loses the time diversity advantage provided by the long time interleaver in time-varying scenarios.

Fig. 2 presents some simulation results for a mobile speed $v = 300$ km/h, hence the corresponding Doppler spread values are doubled with respect to Fig. 1. From Fig. 2 we observe that, at low SNR, DVB-H with LI is capable to achieve better BER performance than T-DMB, when the two systems employ the same $r = 2/3$ convolutional code. However, the overall DVB-H BER performance is worse in practical SNR ranges, due to higher channel estimation errors. Indeed, the BER penalty jointly induced by ICI and channel estimation errors, is highly

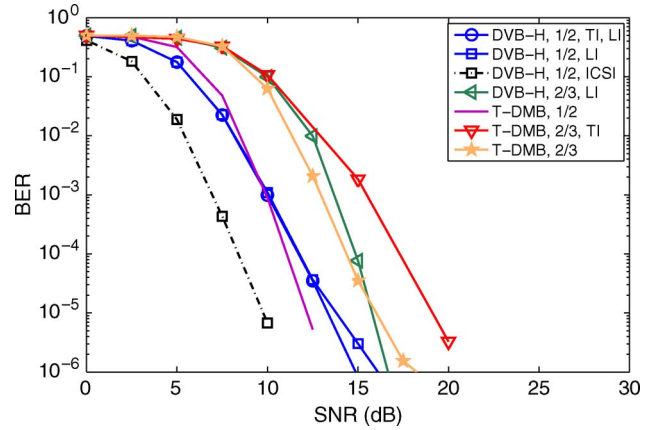


Fig. 1. BER performance of DVB-H at 8 MHz and T-DMB, at the output of the Viterbi decoder (inner BER, i.e., excluding outer RS coding). Rayleigh BU channel, $f_C = 800$ MHz, $v = 150$ km/h ($\bar{f}_D = 0.019$ for T-DMB, $\bar{f}_D = 0.025$ for DVB-H). For TI cases, $v = 0$ km/h.

reduced using LS channel estimation, which is able to capture the performance advantage of DVB-H at any practical SNR. As a result, DVB-H with LS channel estimation significantly outperforms T-DMB. Since we are considering the performance at the output of the Viterbi decoder, it is interesting to focus on the typical target BER $2 \cdot 10^{-4}$, which would correspond to the quasi-error-free (QEF) performance for the MPEG-2 layer in the DVB-T standard [1]. In this case, DVB-H with LI has roughly the same BER of T-DMB, while LS and CI can both provide 1 dB of SNR advantage. Moreover, we observe that, as in Fig. 1, the BER performance of T-DMB with $r = 1/2$ is similar to that of DVB-H with LI and $r = 1/2$; on the other hand, when $r = 2/3$, T-DMB performs worse than DVB-H with LS. This confirms that DVB-H tends to outperform T-DMB in this scenario. We remark that the BER could be further reduced by the outer RS codes, as will be evident in the next figures. Note that in this scenarios the DVB-T BER performance is very close to DVB-H one.

Figs. 1 and 2 also highlight how the channel estimation technique affects the DVB-H BER performance. Specifically, while DVB-H with LI channel estimation performs similarly to

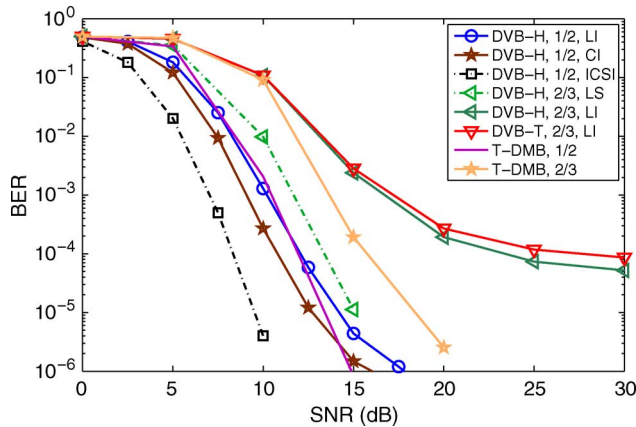


Fig. 2. BER performance of DVB-H at 8 MHz and T-DMB, at the output of the Viterbi decoder (inner BER, i.e., excluding outer RS coding). Rayleigh BU channel, $f_C = 800$ MHz, $v = 300$ km/h ($\bar{f}_D = 0.038$ for T-DMB, $\bar{f}_D = 0.050$ for DVB-H).

T-DMB, using LS (or CI) is highly beneficial and consents to outperform T-DMB. The capability of DVB-H to outperform T-DMB could be surprising, because T-DMB has a smaller normalized Doppler spread \bar{f}_D than DVB-H, and hence a reduced ICI power, and also because the T-DMB interleaver is much longer. The reason is that T-DMB adopts a DQPSK modulation, which is not well suited for fast time-varying channels, where the channel has significantly changed after a single OFDM block duration. From our comparison, we can conclude that the SNR penalty of T-DMB due to the time-domain differential (noncoherent) demodulation is more significant than the gain given by the reduced ICI power and by the increased time diversity. This is also due to the long PDP of the Rayleigh BU channel that supplies a considerable frequency diversity and partially compensates for the reduced time diversity of DVB-T/H caused by the shorter interleaver.

Figs. 3 and 4 illustrate the BER performance of DVB-H on the Rayleigh BU channel for the same speeds of Figs. 1 and 2, using different channel estimation techniques, and convolutional CR $r = 1/2$. We include the BER of the inner DVB-H codec, as well as the BER after outer RS coding. Also in this scenario, the BER of DVB-T is not shown because it is indistinguishable from that of DVB-H. We observe that the effect of the ICI on the Viterbi BER performance is noticeable only for very low BER, well below the QEF threshold $2 \cdot 10^{-4}$. Figs. 3 and 4 also show that the channel estimation method has a significant impact on the BER performance. Therefore, the effect of channel estimation errors can be more relevant than the effect of the ICI induced by Doppler spread. Specifically, in this scenario, LS estimation provides an SNR gain of roughly 1 dB with respect to the simple LI.

For comparison purposes, Fig. 4 also shows the BER in a Rice RA channel with Rice factor $K = 5$ dB, for an inner DVB-H system at $v = 300$ km/h. Surprisingly, it can be noted that, despite the moderately high Rice factor, the BER is much higher than in Rayleigh BU channels, because of the reduced frequency diversity due to the lower delay spread of the RA channel. This behavior will be highlighted also in the next subsection.

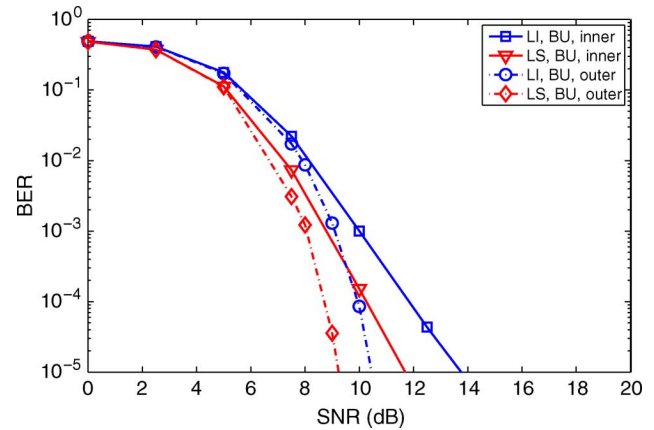


Fig. 3. BER performance of DVB-H at 8 MHz, at the output of the Viterbi decoder (inner) and of the outer RS decoder. Convolutional CR $r = 1/2$, Rayleigh BU channel, $f_C = 800$ MHz, $v = 150$ km/h ($\bar{f}_D = 0.025$).

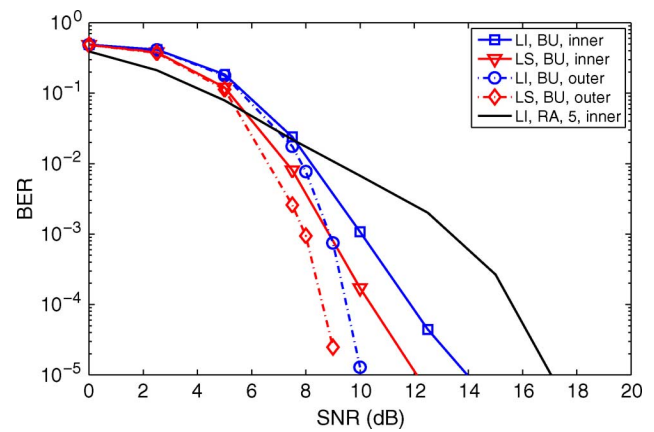


Fig. 4. BER performance of DVB-H at 8 MHz, at the output of the Viterbi decoder (inner) and of the outer RS decoder. Convolutional CR $r = 1/2$, Rayleigh BU or Rice RA channel with $K = 5$ dB, $f_C = 800$ MHz, $v = 300$ km/h ($\bar{f}_D = 0.050$).

B. Rice Channels With Low Delay Spread

Similarly to Figs. 3 and 4, Figs. 5 and 6 display the BER of DVB-H systems in RA channels with Rice factor $K = 0$ dB, for $v = 150$ km/h and $v = 300$ km/h, respectively. Evidently, there exists a performance degradation of DVB-H in RA channels. Moreover, despite the augmented ICI, we can observe a better BER performance for higher Doppler spreads. This apparently strange behavior can be explained by the fact that wireless channels with short delay spreads as the COST 207 RA are represented by few taps in the discrete delay domain (from 4 to 7 for DVB-T/H, 2 for T-DMB). Thus, the consequent high correlation in the frequency domain can largely degrade the DVB-T/H BER performance. In fact, the high correlation between contiguous subcarriers of a single OFDM symbol makes the frequency interleaver scarcely effective, leading to the presence of error bursts that degrade the correcting capability of convolutional codes [38]. This means that the fading experienced by the system, in the absence of an effective (long) time interleaver, becomes similar to a block fading. Summarizing, the DVB-H performance loss in RA with respect to BU is, obviously, not

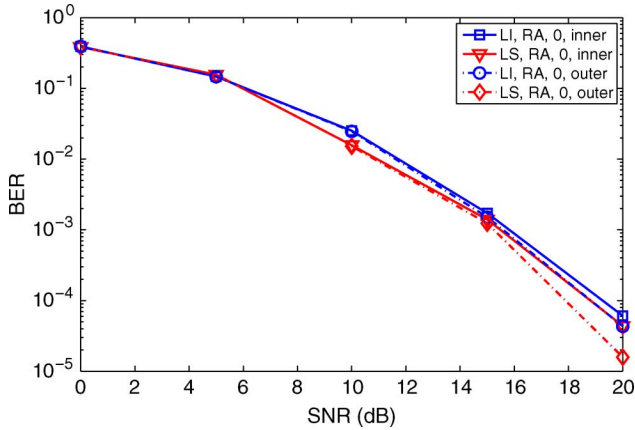


Fig. 5. BER performance of DVB-H at 8 MHz, at the output of the Viterbi decoder (inner) and of the outer RS decoder. Convolutional CR $r = 1/2$, Rice RA channel with $K = 0$ dB, $f_C = 800$ MHz, $v = 150$ km/h ($\bar{f}_D = 0.025$).

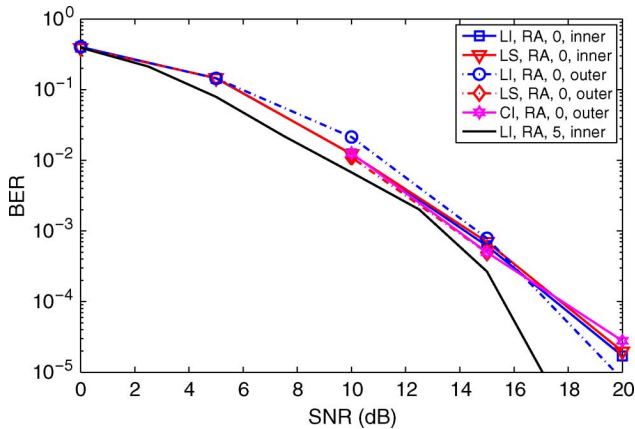


Fig. 6. BER performance of DVB-H at 8 MHz, at the output of the Viterbi decoder (inner) and of the outer RS decoder. Convolutional CR $r = 1/2$, Rice RA channel with $K = 0$ dB or $K = 5$ dB, $f_C = 800$ MHz, $v = 300$ km/h ($\bar{f}_D = 0.050$).

due to the greater LOS path, but it is caused by the frequency diversity loss produced by lower delay spreads.

Figs. 7 and 8 exhibit the BER performance, at the output of the RS decoder, of T-DMB and DVB-H (at 5 MHz) on a Rice RA channel with Rice factor $K = 10$ dB, when $v = 150$ and $v = 300$ km/h. Now we assume that the carrier frequency is $f_C = 1.4$ GHz, which leads to $\bar{f}_D \approx 3.4\%$ and $\bar{f}_D \approx 6.7\%$ for T-DMB, and $\bar{f}_D \approx 7.0\%$ and $\bar{f}_D \approx 13.9\%$ for DVB-H. We observe that T-DMB largely outperforms DVB-H at high SNR, because of the longer time interleaving. On the other hand, at low SNR, DVB-H outperforms T-DMB. Moreover, by increasing the speed from $v = 150$ to $v = 300$ km/h, DVB-H shows improved BER performance, because the enhanced time diversity exploited by the outer interleaver counterbalances the BER degradation induced by the ICI power increase. Indeed, when $v = 300$ km/h, DVB-H outperforms T-DMB not only at low SNR, but also at medium SNR. In addition, it is evident that also in this scenario the LS channel estimation provides a significant SNR gain (about 2 dB) with respect to LI. These results confirm that the type of channel estimation plays a relevant role in determining the DVB-T/H performance. Note also that, although

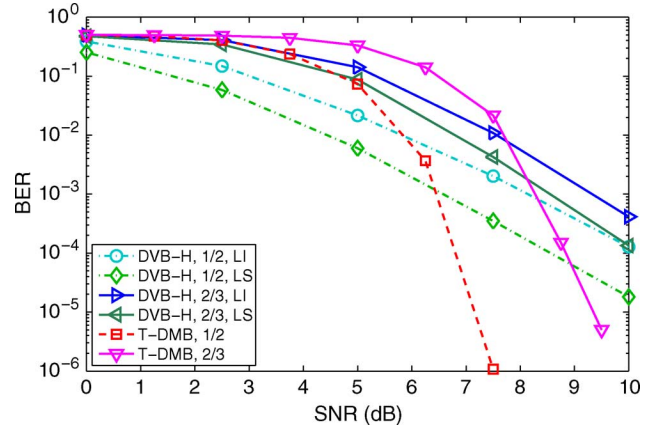


Fig. 7. BER performance of DVB-H at 5 MHz and T-DMB, at the output of the outer RS decoder. Rice RA channel with $K = 10$ dB, $f_C = 1.4$ GHz, $v = 150$ km/h ($\bar{f}_D = 0.034$ for T-DMB, $\bar{f}_D = 0.070$ for DVB-H).

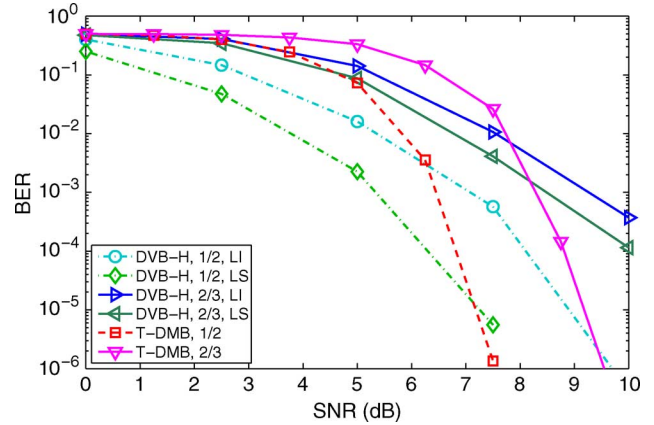


Fig. 8. BER performance of DVB-H at 5 MHz and T-DMB, at the output of the outer RS decoder. Rice RA channel with $K = 10$ dB, $f_C = 1.4$ GHz, $v = 300$ km/h ($\bar{f}_D = 0.067$ for T-DMB, $\bar{f}_D = 0.139$ for DVB-H).

not shown in Figs. 7 and 8, DVB-T in this scenarios slightly underperforms DVB-H.

Figs. 9 and 10 present the BER performance of T-DMB and DAB (i.e., inner T-DMB) for the Rice RA channel with $K = 0$ dB and for the Rayleigh BU channel, assuming a CR $r = 1/2$ and $r = 2/3$, respectively. We observe that, differently from the DVB-H performances of Figs. 3–6, the RS code of T-DMB is always very effective, in both Rayleigh and Rice channels. Indeed, although T-DMB experiences less frequency diversity than DVB-H, the very long time interleaver of T-DMB captures great part of the time diversity offered by the channel, reducing the BER sensitivity to the PDP, especially for high values of Doppler spread. In particular, such a long interleaver, which spans 2160 OFDM symbols, makes it possible to consider the channel almost ergodic, enabling for T-DMB the good correcting capability of the RS code, which, contrarily to what happens with DVB-T, greatly mitigates a deep channel fade. As a consequence, the BER curves for T-DMB in Rice and Rayleigh channels follow similar trends, provided that the Rice factor is modest. In a nutshell, the lower sensitivity of T-DMB to the channel delay spread produces a performance gain with respect to DVB-T/H when the frequency diversity is limited.

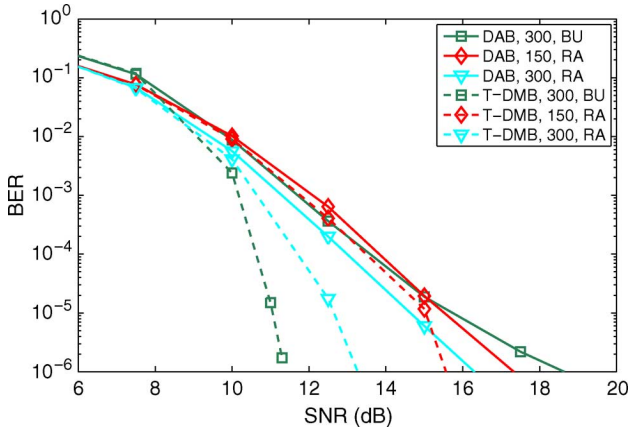


Fig. 9. BER performance of T-DMB at the output of the Viterbi decoder (DAB) and of the outer RS decoder. Rayleigh BU or Rice RA channel with $K = 0$ dB, $f_C = 1.4$ GHz, $\mathbf{CR} r = 1/2$, $v = 150$ km/h ($\bar{f}_D = 0.034$) and $v = 300$ km/h ($\bar{f}_D = 0.067$).

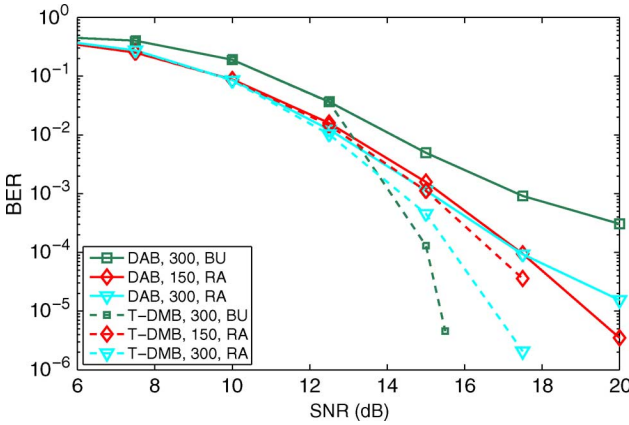


Fig. 10. BER performance of T-DMB at the output of the Viterbi decoder (DAB) and of the outer RS decoder. Rayleigh BU or Rice RA channel with $K = 0$ dB, $f_C = 1.4$ GHz, $\mathbf{CR} r = 2/3$, $v = 150$ km/h ($\bar{f}_D = 0.034$) and $v = 300$ km/h ($\bar{f}_D = 0.067$).

Although we mainly focus on the PHY layer, we now turn our attention to the DL layer performance of DVB-H, which includes a further coding protection denoted with MPE-FEC. Fig. 11 displays the BER performance at the output of the MPE-FEC decoder for a DVB-H system which employs a simple LI channel estimation, assuming a Rice RA channel with Rice factor K . This scenario is particularly challenging for DVB-H systems, because of the scarce frequency diversity. We remark that the MPE-FEC is an RS code with $\mathbf{CR} r_{MPE-FEC} = 191/255$, and consequently the DL layer efficiency η_{DL} of DVB-H is roughly 0.75 times the PHY layer spectral efficiency η .

Fig. 11 shows that in all the considered scenarios the MPE-FEC is highly effective in reducing the error rate. Specifically, MPE-FEC counterbalances the lack of temporal diversity of DVB-H caused by the short inner interleaver. Indeed, when the MPE-FEC interleaver acts on 1024 codewords, the interleaver depth is about 1519 OFDM blocks. Therefore, thanks to the additional coding, DVB-H with LI channel estimation is able to perform similarly to T-DMB also in Rice RA channels with low delay spread. For instance, by comparing Fig. 11

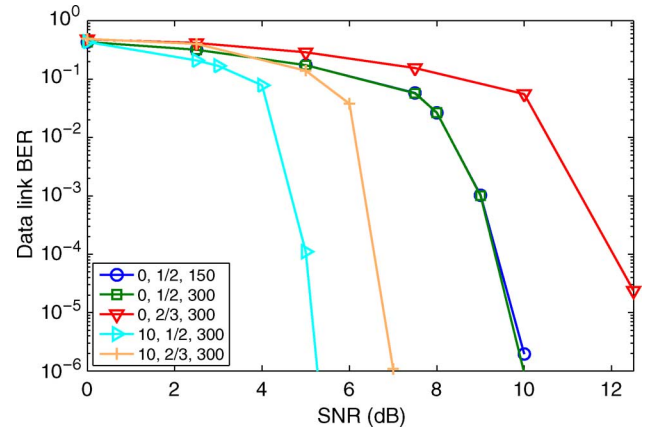


Fig. 11. DL layer BER performance of DVB-H at 8 MHz at the output of the MPE-FEC decoder. Rice RA channel with $K = 0$ dB or $K = 10$ dB, $f_C = 1.4$ GHz, convolutional $\mathbf{CR} r = 1/2$ or $r = 2/3$, $v = 150$ km/h ($\bar{f}_D = 0.025$) or $v = 300$ km/h ($\bar{f}_D = 0.050$).

with Fig. 9, when $K = 0$ dB and $v = 300$ km/h, for a target BER of 10^{-5} , DVB-H with LI and convolutional $\mathbf{CR} r = 2/3$ ($\eta_{DL} \approx 0.77$) performs similarly to T-DMB with $r = 1/2$ ($\eta \approx 0.74$). In the same scenario, DVB-H outperforms T-DMB at lower BER, whereas T-DMB outperforms DVB-H at greater BER. However, it should be noted that DVB-H is employing the simple LI channel estimation and hence its performance can be improved further, as shown in Figs. 5 and 6. From Fig. 11, we also observe that the performance of DVB-H with MPE-FEC when $v = 150$ km/h is practically identical to that obtained when $v = 300$ km/h: this behavior also happens in the three cases not shown in Fig. 11, i.e., when $K = 10$ and when $r = 2/3$. Moreover, additional information about the performance of MPE-FEC can be obtained, e.g., in [14], [16].

C. Spatial Diversity

We now focus on the effect of using two receive antennas, where ρ denotes the correlation coefficient. Obviously, when $\rho = 1$, there is no spatial diversity, since the channels are identical. However, when $\rho = 1$, both MRC and EGC supply a 3 dB SNR gain, because the two useful signals add constructively, while the two independent noise terms add incoherently. As far as DVB-T/H systems are concerned, we only consider DVB-T with LI, because this is the worst scenario, i.e., the scenario that mainly requires a performance improvement. Therefore, this scenario is particularly suitable to show the great diversity gain that can be achieved using two receive antennas. Moreover, since LI is the easiest channel estimation, any practical DVB-T receiver should perform better or equal in respect of channel estimation. As explained in Section V, MRC (16) is used for DVB-T, while EGC (17) is employed for T-DMB.

Fig. 12 presents the inner BER of T-DMB (i.e., DAB) with convolutional $\mathbf{CR} r = 2/3$ and the inner BER of DVB-T with LI and $r = 1/2$, assuming Rayleigh BU channels in a high-mobility scenario ($v = 300$ km/h). These results clearly point out the beneficial impact of multiple receive antennas on the performance. Noteworthy, the spatial diversity greatly reduces the effect of the ICI, leading to a reduced BER floor. Although the diversity gain is maximum for uncorrelated channels, where

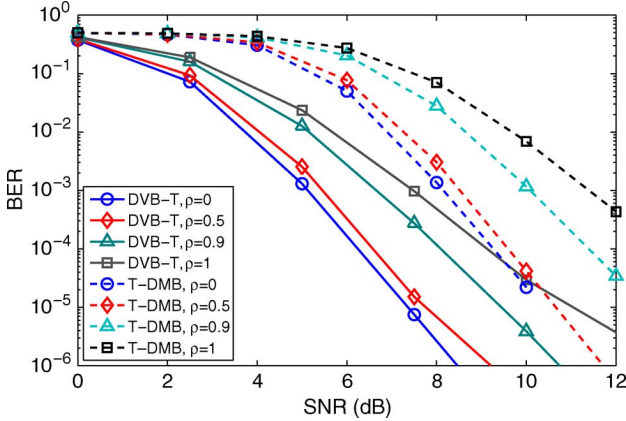


Fig. 12. BER performance of DVB-T at 8 MHz with $r = 1/2$ and T-DMB (DAB) with $r = 2/3$ at the output of the Viterbi decoder, for two receive antennas. **Rayleigh BU** channel, $f_C = 800$ MHz, $v = 300$ km/h ($\bar{f}_D = 0.038$ for T-DMB, $\bar{f}_D = 0.050$ for DVB-T).

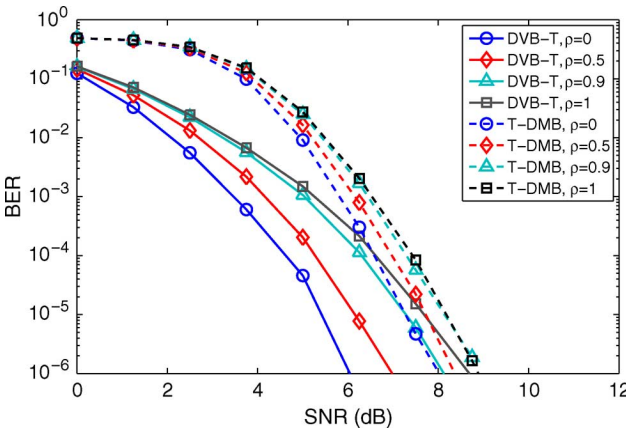


Fig. 13. BER performance of DVB-T at 8 MHz with $r = 1/2$ and T-DMB (DAB) with $r = 2/3$ at the output of the Viterbi decoder, for two receive antennas. **Rice RA** channel with $K = 10$ dB, $f_C = 800$ MHz, $v = 300$ km/h ($\bar{f}_D = 0.038$ for T-DMB, $\bar{f}_D = 0.050$ for DVB-T).

$\rho = 0$, our simulations interestingly show that for DVB-T there is a substantial performance gain even for highly correlated channels, i.e., when $\rho = 0.9$; this result should greatly push manufacturers to exploit multiple antennas. In the case of T-DMB, we observe a diversity behavior similar to DVB-T in uncorrelated channels.

The BER curves of Fig. 13 are obtained in a scenario similar to Fig. 12, assuming a Rice RA channel with $K = 10$ dB. Fig. 13 reveals that Rice channels lead to improved BER performance with respect to the Rayleigh case of Fig. 12. This result is consistent with those obtained from single-antenna receivers. However, it should be noted that, differently from Fig. 12, Fig. 13 does not exhibit any BER floor, at least when the BER exceeds 10^{-7} . Indeed, in the Rice case, the power of the random part of the channel is reduced with respect to the Rayleigh case. Therefore, the ICI power is reduced too. In addition, with respect to Fig. 12, in Fig. 13 the BER curves for different values of ρ are closer to each other. In fact, when the Rice factor is high, the mean value of the first path of the channel is high. As a consequence, it is easy to verify that

the statistical correlation between the first paths (i.e., those with LOS) of the two channels is quite significant even when the correlation coefficient ρ (i.e., the covariance) is zero. This high correlation is responsible for the similar performances at different values of ρ .

Another observation derived from Figs. 12 and 13 is related to the effect of the correlation coefficient ρ . Specifically, in the Rayleigh case of Fig. 12, the BER in moderately correlated channels ($\rho = 0.5$) is close to the BER in uncorrelated channels, while in the Rice case of Fig. 13 there is a non-negligible performance gap. Furthermore, differently from Fig. 12, in Fig. 13 the BER in heavily correlated channels ($\rho = 0.9$) is very close to the BER in maximally correlated channels ($\rho = 1$). Therefore, we can conclude that the impact of the channel correlation on the ultimate BER performance seems to be different for Rice and Rayleigh channels: this is partially surprising as evidenced in [39].

VII. CONCLUSIONS

To the best of our knowledge, this is the first paper that has presented a detailed comparison of the coded BER performance in high-mobility scenarios of two popular broadcasting standards, DVB-T/H and T-DMB. Focusing on Rice and Rayleigh doubly-selective fading channels, we have illustrated that DVB-T/H and T-DMB (and DAB) behave differently as the channel type changes. First, the DVB-H performance highly depends on the delay spread of the channel, while T-DMB is much less sensitive to the delay spread. Indeed, in T-DMB, the limited frequency diversity of low delay-spread channels is compensated by the higher time diversity provided by the long time interleaver. In a nutshell, DVB-H outperforms T-DMB in Rayleigh channels with high delay spread. On the contrary, at high SNR, T-DMB generally outperforms DVB-H in Rice channels with low delay spread. It is worth noting, however, that MPE-FEC highly improves the DVB-H performance.

In our comparison, we have also included the effect of different channel estimation techniques for DVB-T/H. We have shown that LS fitting leads to a BER performance close to that obtained with ideal channel knowledge. On the other hand, the SNR penalty produced by LI can be justified by the simplicity of interpolation. In the middle, CI represents an alternative and appealing technique with both good performance and moderate complexity.

We have also shown that spatial diversity can greatly boost the BER performance also in time-varying scenarios. Simulation results for DVB-T/H with MRC and for T-DMB with EGC have been presented for two receive antennas. Interestingly, the performance gain given by two receive antennas remains significant, also when the channels are correlated. This means that improved performance is feasible even using small-size mobile terminals.

As a concluding remark, we believe that this thorough and fair analysis and comparison, though mainly focused on the PHY layer, can clarify, to system designers and operators, the specific merits of the two systems, highlighting the main performance differences in mobile channels.

REFERENCES

- [1] *Digital Video Broadcasting (DVB); Framing Structure, Channel Coding and Modulation for Digital Terrestrial Television*, ETSI EN 300 744 V1.5.1, ETSI, Nov. 2004.
- [2] M. Kornfeld and G. May, "DVB-H and IP datacast-broadcast to handheld devices," *IEEE Trans. Broadcast.*, vol. 53, no. 1, pp. 161–170, Mar. 2007.
- [3] *Radio Broadcasting Systems; Digital Audio Broadcasting (DAB) to Mobile, Portable and Fixed Receivers*, ETSI EN 300 401 V1.3.3, ETSI, May 2001.
- [4] *Digital Audio Broadcasting (DAB); Data Broadcasting—MPEG-2 TS Streaming*, ETSI TS 102 427 V1.1.1, ETSI, Jul. 2005.
- [5] S. Cho, G. S. Lee, B. Bae, K. T. Yang, C.-H. Ahn, S.-I. Lee, and C. Ahn, "System and services of Terrestrial Digital Multimedia Broadcasting (T-DMB)," *IEEE Trans. Broadcast.*, vol. 53, no. 1, pp. 171–178, Mar. 2007.
- [6] P. Hoher, J. Hagenauer, E. Offer, C. Rapp, and H. Schulze, "Performance of an RCPC-coded OFDM-based digital audio broadcasting (DAB) system," in *Proc. IEEE Global Telecommun. Conf. 1991 (GLOBECOM'91)*, Phoenix, AZ, Dec. 2–5, 1991, vol. 1, pp. 40–46.
- [7] R. Burow, K. Fazel, P. Hoehner, O. Klank, H. Kussmann, P. Pogrzeba, P. Robertson, and M. J. Ruf, "On the performance of the DVB-T system in mobile environments," in *Proc. IEEE Global Telecommun. Conf. 1998 (GLOBECOM'98)*, Sydney, Australia, Nov. 8–12, 1998, vol. 4, pp. 2198–2204.
- [8] J. Jootar, J. R. Zeidler, and J. G. Proakis, "Performance of convolutional Codes with finite-depth interleaving and noisy channel estimates," *IEEE Trans. Commun.*, vol. 54, no. 10, pp. 1775–1786, Oct. 2006.
- [9] G. Zimmermann, M. Rosenberger, and S. Dostert, "Theoretical bit error rate for uncoded and coded data transmission in digital audio broadcasting," in *Proc. IEEE Int. Conf. Commun. 1996 (ICC'96)*, Dallas, TX, Jun. 23–27, 1996, vol. 1, pp. 297–301.
- [10] A. G. Armada, B. Bardon, and M. Calvo, "Parameter optimization and simulated performance of a DVB-T digital television broadcasting system," *IEEE Trans. Broadcast.*, vol. 44, no. 1, pp. 131–138, Mar. 1998.
- [11] S. Tomasin, A. Gorokhov, H. Yang, and J.-P. Linnartz, "Reduced complexity Doppler compensation for mobile DVB-T," in *Proc. IEEE Personal, Indoor and Mobile Radio Commun. 2002 (PIMRC'02)*, Lisbon, Portugal, Sep. 15–18, 2002, vol. 5, pp. 2077–2081.
- [12] M. Velez, D. de la Vega, P. Angueira, D. Guerra, G. Prieto, and A. Arrinda, "Field measurement based performance analysis of digital audio broadcasting (DAB) reception in mobile channels," in *IEEE Veh. Technol. Conf. 2005 Spring (VTC'05-Spring)*, Stockholm, Sweden, May 30–Jun. 1 2005, vol. 1, pp. 247–251.
- [13] Y. J. Lee, S. W. Lee, Y. H. Kim, S. I. Lee, Z.-K. Yim, B. H. Choi, S. J. Kim, and J.-S. Seo, "Field trials for Terrestrial Digital Multimedia Broadcasting system," *IEEE Trans. Broadcast.*, vol. 53, no. 1, pp. 425–433, Mar. 2007.
- [14] J. Paavola, H. Himmanen, T. Jokela, J. Poikonen, and V. Ipatov, "The performance analysis of MPE-FEC decoding methods at the DVB-H link layer for efficient IP packet retrieval," *IEEE Trans. Broadcast.*, vol. 53, no. 1, pp. 263–275, Mar. 2007.
- [15] W. Joseph, D. Plets, L. Verloock, E. Tanghe, L. Martens, E. Deventer, and H. Gauderis, "Procedure to optimize coverage and throughput for a DVB-H system based on field trials," *IEEE Trans. Broadcast.*, vol. 54, no. 3, pp. 347–355, Sep. 2008.
- [16] D. Plets, W. Joseph, L. Verloock, E. Tanghe, L. Martens, E. Deventer, and H. Gauderis, "Influence of reception condition, MPE-FEC rate and modulation scheme on performance of DVB-H," *IEEE Trans. Broadcast.*, vol. 54, no. 3, pp. 590–598, Sep. 2008.
- [17] Y. Wu, E. Pliszka, B. Caron, P. Bouchard, and G. Chouinard, "Comparison of terrestrial DTV transmission systems: The ATSC 8-VSB, the DVB-T COFDM, and the ISDB-T BST-OFDM," *IEEE Trans. Broadcast.*, vol. 46, no. 2, pp. 101–113, Jun. 2000.
- [18] E. Chiavaccini and G. Vitetta, "Error performance of OFDM signaling over doubly-selective Rayleigh fading channels," *IEEE Commun. Lett.*, vol. 4, no. 11, pp. 328–330, Nov. 2000.
- [19] M. Poggioni, L. Rugini, and P. Banelli, "A novel simulation model for coded OFDM in Doppler scenarios," *IEEE Trans. Veh. Technol.*, vol. 57, no. 5, pp. 2969–2980, Sep. 2008.
- [20] M. Lentmaier, D. V. Truhachev, and K. S. Zigangirov, "Analytic expressions for the bit error probabilities of rate-1/2 memory 2 convolutional encoders," *IEEE Trans. Inf. Theory*, vol. 50, no. 6, pp. 1303–1311, Jun. 2004.
- [21] E. Malkamäki and H. Leib, "Evaluating the performance of convolutional codes over block fading channels," *IEEE Trans. Inf. Theory*, vol. 45, no. 5, pp. 1643–1646, Jul. 1999.
- [22] P. Bello, "Characterization of randomly time-variant linear channels," *IEEE Trans. Commun. Syst.*, vol. 11, no. 4, pp. 360–393, Dec. 1963.
- [23] Z. Wang and G. Giannakis, "Wireless multicarrier communications," *IEEE Signal Process. Mag.*, vol. 17, no. 3, pp. 29–48, May 2000.
- [24] M. Russell and G. Stüber, "Interchannel interference analysis of OFDM in a mobile environment," in *IEEE Veh. Technol. Conf. 1995 (VTC'95)*, Chicago, IL, Jul. 25–28, 1995, vol. 2, pp. 820–824.
- [25] Digital Land Mobile Radio Communications COST 207 European Commission, 1989, Tech. Rep..
- [26] Y. R. Zheng and C. Xiao, "Improved models for the generation of multiple uncorrelated Rayleigh fading waveforms," *IEEE Commun. Lett.*, vol. 6, no. 6, pp. 256–258, Jun. 2002.
- [27] M. Poggioni, L. Rugini, and P. Banelli, "A novel simulation model for coded OFDM in Doppler scenarios: DVB-T versus DAB," in *Proc. IEEE Int. Conf. Commun. 2007 (ICC'07)*, Glasgow, UK, Jun. 24–28, 2007, pp. 5689–5694.
- [28] Z. Tang, R. C. Cannizzaro, G. Leus, and P. Banelli, "Pilot-assisted time-varying channel estimation for OFDM systems," *IEEE Trans. Signal Process.*, vol. 55, no. 5, pp. 2226–2238, May 2007.
- [29] M. Morelli and U. Mengali, "A comparison of pilot-aided channel estimation methods for OFDM systems," *IEEE Trans. Signal Process.*, vol. 49, no. 12, pp. 3065–3073, Dec. 2001.
- [30] S.-H. Kim, Y.-S. Kim, J.-S. Lim, C. Ahn, U.-R. Choi, and B.-S. Soe, "Design of the channel estimation algorithm for advanced terrestrial DMB system," *IEEE Trans. Broadcast.*, vol. 54, no. 4, pp. 816–820, Dec. 2008.
- [31] F. Sanzi and J. Speidel, "An adaptive two-dimensional channel estimator for wireless OFDM with application to mobile DVB-T," *IEEE Trans. Broadcast.*, vol. 46, no. 2, pp. 128–133, Jun. 2000.
- [32] M. K. Ozdemir and H. Arslan, "Channel estimation for wireless OFDM systems," *IEEE Commun. Surveys Tuts.*, vol. 9, no. 2, pp. 18–48, 2nd Quarter 2007.
- [33] S. M. Kay, *Fundamentals of Statistical Signal Processing: Estimation Theory*. Upper Saddle River, NJ, USA: Prentice-Hall, Inc., 1993.
- [34] W.-C. Lee, H.-M. Park, and J. S. Park, "Viterbi decoding method using channel state information in COFDM system," *IEEE Trans. Consum. Electron.*, vol. 45, no. 3, pp. 533–537, Aug. 1999.
- [35] A. Dammann and S. Kaiser, "Transmit/receive-antenna diversity techniques for OFDM systems," *European Trans. Telecommun.*, vol. 13, no. 5, pp. 531–538, 2002.
- [36] M.-S. Baek, M.-J. Kim, Y.-H. You, and H.-K. Song, "Design and performance evaluation of {DAB} system with multiple antennas," in *IEEE Veh. Technol. Conf. 2004 Fall (VTC'04-Fall)*, Los Angeles, CA, Sep. 26–29, 2004, vol. 7, pp. 4663–4667.
- [37] D. Brennan, "Linear diversity combining techniques," *Proc. IRE*, vol. 47, no. 6, pp. 1075–1102, June 1959.
- [38] J. G. Proakis, *Digital Communications*, 4th ed. New York: McGraw-Hill, 2000.
- [39] Y. Ma, T. L. Lim, and S. Pasupathy, "Error probability for coherent and differential PSK over arbitrary Rician fading channels with multiple cochannel interferers," *IEEE Trans. Commun.*, vol. 50, no. 3, pp. 429–441, Mar. 2002.



Mario Poggioni (S'07) was born in Perugia, Italy, in 1979. He received the Laurea degree (magna cum laude) in electronics engineering in 2005 and the Ph.D. degree in telecommunications in 2009, from the University of Perugia. He is currently a Research Engineer with ART Srl. His research interests lie in the area of signal processing for multicarrier communications, fast fading channels, broadcasting and cross-layer designs.



spread-spectrum communications.

Luca Rugini (S'01–M'05) was born in Perugia, Italy, in 1975. He received the Laurea degree in electronic engineering and the Ph.D. degree in telecommunications from the University of Perugia, in 2000 and 2003, respectively. From February to July 2007, he visited Delft University of Technology, The Netherlands. He is currently an Assistant Professor with the Department of Electronic and Information Engineering at the University of Perugia. His research interests lie in the area of signal processing for multicarrier and



His research interests mainly focus on signal processing for wireless communications, with emphasis on multicarrier transmissions, and more recently on signal processing for biomedical applications, with emphasis on electrocardiography and medical ultrasounds. He has been serving as a Reviewer for several technical journals, as technical program committee member of leading international conferences on signal processing and telecommunications. He was a General Co-Chair of the IEEE International Symposium on Signal Processing Advances for Wireless Communications 2009.

Paolo Banelli (S'90–M'99) received the Laurea degree in electronics engineering and the Ph.D. degree in telecommunications from the University of Perugia, Perugia, Italy, in 1993 and 1998, respectively. In 2005, he was appointed Associate Professor at the Department of Electronic and Information Engineering (DIEI), University of Perugia, where he has been an Assistant Professor since 1998. In 2001, he joined the SpinComm group at the Electrical and Computer Engineering Department, University of Minnesota, Minneapolis, as a Visiting Researcher.